A Joint Lidar Solar Radiometer Experiment

G. S. KENT

Physics Department, University of the West Indies, Kingston 1, Jamaica

F. KÖPP AND CH. WERNER

Institute of Atmospheric Physics, German Aerospace Establishment (DFVLR), D-8031 Oberpfaffenhofen, Federal Republic of Germany

(Manuscript received 12 April 1979, in final form 27 August 1979)

ABSTRACT

Remote sensing of the lower atmosphere by lidar yields profiles of the backscattering cross section along the optical path. These may be simply converted to give a qualitative picture of the distribution of atmospheric aerosol, but quantitative values can only be obtained if further information is available on aerosol properties such as refractive index and size distribution. In the experiments described below, use was made of a solar radiometer to give information on the second of these. This is then used to calculate an improved value for the ratio of backscattering to aerosol mass (β/m) for the interpretation of the lidar data. Comparison is made of the results of radiometer measurements, taken at a rural area outside Munich, with airborne lidar measurements of the tropospheric aerosol made in the same locality. Aerosol density profiles obtained in another flight made near Augsburg on 22 July 1977 show the presence of a heavy aerosol concentration over the city and the effects of the north wind are clearly visible.

1. Introduction

Remote sensing of atmospheric aerosols by lidar systems primarily yields profiles of backscattering cross sections which give a qualitative indication of the aerosol distribution along the optical path. A further step is the transformation of the backscatter data into aerosol mass concentrations which may have large uncertainties caused by the complex dependence of the scattering cross sections on aerosol type and size distribution. The aim of the Joint Lidar-Solar-Radiometer Experiment described here was to improve the accuracy of mass concentrations derived from aerosol lidar measurements, using information derived from simultaneous radiometer measurements.

It has been shown by Kent (1978) that the high uncertainties arising from measurements with a one-wavelength lidar system can be reduced if information is available, or assumptions can be made, about the aerosol size distribution. For further improvement simultaneous lidar measurements at different wavelengths are recommended. Since in our case, a multi-wavelength lidar system was not available, alternative use was made of a multi-wavelength radiometer. Using measurements over a range of wavelengths it was possible to determine the relative number of aerosol particles in the coarse particle and accumulation modes. Given a value for this ratio, it is then possible to estimate, with greater precision, the ratio of aerosol backscattering cross section β, at the lidar wavelength, to the aerosol mass concentration.

2. Single-wavelength lidar measurements

a. Description of the lidar system

The lidar measurements for the joint experiment were carried out with the same system as used during the ASSESS II Mission (Airborne Science Spacelab Experiments System Simulation). Since a detailed description of this system has been given by Werner *et al.* (1978), we may restrict ourselves to basic technical data.

The lidar mainly consists of a Nd:glass laser as transmitter and a parabolic mirror as receiver. The backscattered signal is directly detected by a photodiode YAG 444, amplified, and stored on a transient recorder Biomation 8100. In Table 1 the parameters of the system are summarized.

For calibration, the lidar was pointing from the ground to the base of a dense, homogeneous stratocumulus layer. The backscatter properties for the lidar wavelength were determined by Mie calculation.

b. Measurement of vertical lidar profiles

For the joint experiment the lidar system was installed in a twin-engined aircraft Do 28 Skyservant from DFVLR. Fig. 1 shows a view into the aircraft

0021-8952/79/121649-07$05.75

TABLE 1. Parameters of the airborne aerosol lidar system.

Transmitter	
Nd: glass laser	Zeiss
Wavelength	1.06 μm
output energy	0.15 J
input energy	120 J (battery operated)
pulse duration	30 ns
pulse repetition rate	⅓ Hz
weight	15 kg
Receiver	
parabolic mirror	60 cm diameter
used area	40 cm diameter
focal length	24 cm
photodiode	YAG 444
(S/N = 1 for $\beta = 10^{-7}$ m^{-1} sr^{-1} at 6.5 km range)	
weight	30 kg

Dimensions: 70 cm × 80 cm, height 50 cm.

in which two 19 inch racks with electronics and tape recorder and a small part of the lidar frame can be seen. The lidar system is mounted above a window in the aircraft floor which can be opened after takeoff. From 19 to 22 July 1977 five flights in the Munich and Augsburg area were carried out. During the flights the backscatter profiles $\beta\tau^2$ from the aircraft down to the ground were measured. After a coarse correction for the extinction losses (τ^2) on the double ray path, the profiles taken at local overflights were compared with the radiometer data measured at the same time. Three measured and corrected lidar profiles from three different days are shown in Fig. 2.

3. Solar radiometer measurements

a. Description of the solar radiometer

The radiometer used was an eight-wavelength filter wheel radiometer developed at the Department of Electrical Engineering, University of Arizona. It is similar to that described by Shaw *et al.* (1973) except that the sequencing of the filters was carried out manually rather than automatically. The interference filters had passbands extending over a wavelength range from 0.3714 to 1.0303 μm, and the instrument was used to measure the relative irradiance of transmitted sunlight arriving at the earth's surface. The fraction of energy passing through each filter was detected on a UDT-10 photodiode and the amplified voltage read manually from a digital voltmeter. The radiometer was fitted with a calibrated thermistor so that the filter temperature could be determined. A correction was applied to the detected voltage at the longest wavelength which showed an appreciable temperature sensitivity.

The measured irradiance of the solar flux is given approximately by the equation (Shaw *et al.*, 1973)

$$F(\lambda,z) = F_0(\lambda) \exp[-\sec z \tau_t(\lambda)], \qquad (1)$$

where $F(\lambda,z)$ is the observed ground level irradiance at wavelength λ and solar zenith angle z, $F_0(\lambda)$ the irradiance above atmosphere at wavelength λ and $\tau_t(\lambda)$ the total optical depth at wavelength λ along the zenith, given by

$$\tau_t(\lambda) = \tau_R(\lambda)\frac{P}{P_0} + \tau_a(\lambda) + \tau_p(\lambda), \qquad (2)$$

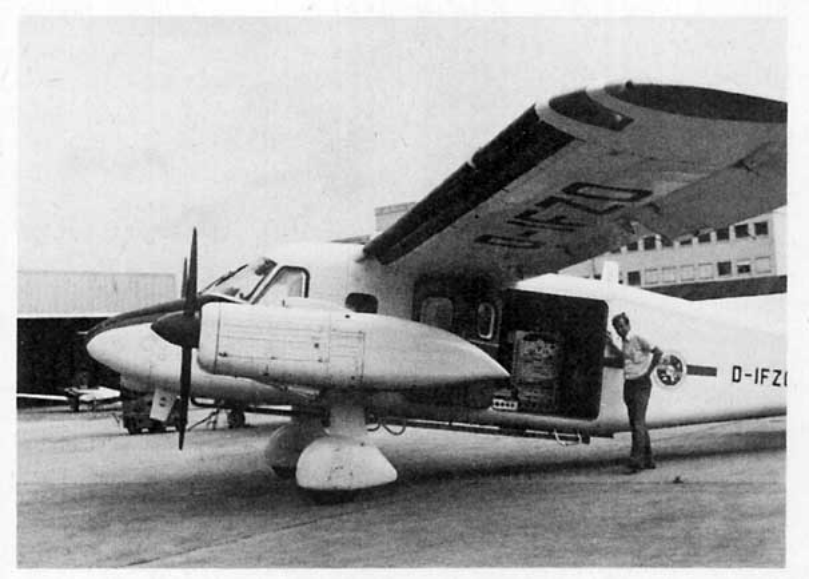

FIG. 1. View into Do 28 aircraft, showing two racks filled with electronics and tape recorder and parts of the lidar frame.

where $\tau_R(\lambda)$ is the optical depth for molecular (Rayleigh) scattering in a standard atmosphere, P the actual atmospheric pressure, P_0 the standard atmospheric pressure, $\tau_a(\lambda)$ the optical depth arising from absorption by atmospheric gases, and $\tau_p(\lambda)$ the optical depth arising from absorption and scattering by atmospheric aerosols. The objective of the measurements described here was the determination of $\tau_p(\lambda)$ at the chosen wavelengths and the use of these values to estimate the atmospheric aerosol content and size distribution. This involves the determination of the other terms entering Eqs. (1) and (2) and the use of the suitable aerosol model to relate $\tau_p(\lambda)$ to the aerosol characteristics. In Eq. (1), the solar zenith angle can be found by calculation, using astronomical tables, from the time of day, date and the latitude and longitude of the observing point. $F(\lambda,z)$ is the measured flux on the radiometer, while $F_0(\lambda)$ must be found by a calibration procedure described briefly below.

b. Calibration of the solar radiometer

In theory, the calibration of the radiometer at each wavelength is a relatively simple matter involving the determination of $F(\lambda,z)$ at various values of secz, the plotting of a suitable semi-logarithmic graph and extrapolation to secz = 0. In practice it involves the assumption that $\tau_t(\lambda)$ does not change appreciably during the period of observation. During the time available for calibration (May–August 1977) very few suitable occasions were obtained even though, for this purpose, the radiometer was taken into mountainous terrain to altitudes above 2000 m. The calibration was eventually taken as the average of the values measured on six occasions when the conditions were considered good enough for use (absence of cloud and haze) and a sufficient range in secz was obtained. The standard deviation of the final values for $F_0(\lambda)$ varied from approximately 2% at 1.03 μm to 6% at 0.37 μm.

c. Calculation of aerosol optical depth

$\tau_t(\lambda)$ is determined by direct calculation from $F(\lambda,z)$, $F_0(\lambda)$ and secz. Values for $\tau_R(\lambda)$ and $\tau_a(\lambda)$ were taken from the *Handbook of Geophysics and Space Environments* (1965), $\tau_a(\lambda)$ being supposed to depend only on the presence of ozone. Allowance was made for the seasonal variation of ozone according to Wilcox *et al.* (1977). No correction has been made for NO_2 absorption which will have increased $\tau_a(\lambda)$ slightly at the shortest wavelengths, particularly at $\lambda = 0.37$ μm. Since all measurements have been made under nonurban conditions, it has been assumed that the NO_2 absorption is small (Shaw, 1976). P was found by direct measurement. Typical values of $\tau_p(\lambda)$ found in this way under clear-sky conditions and altitudes below 1000 m varied from approximately 0.1 at 1.03 μm to 0.4 at 0.37 μm.

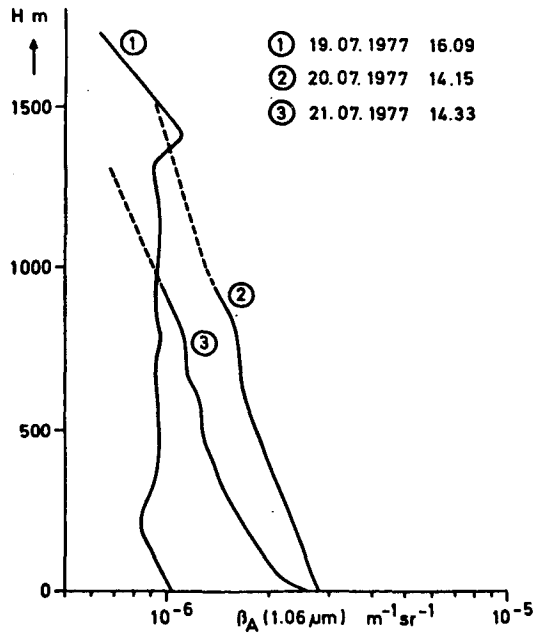

FIG. 2. Aerosol backscatter profiles measured with the airborne lidar system. Dashed parts of curves 2 and 3 have been extrapolated up to the inversion height.

d. Observations made

Observations were made as part of the joint experiment on 19, 20 and 21 July 1977. These were taken under conditions of patchy cumulus clouds, with measurements being made only when the sun appeared in a clear sky well away from the nearest cloud. Due to heavier cloud, no observations were possible on 22 July. All observations were made from the Institute of Atmospheric Physics, DFVLR, Oberpfaffenhofen (48.1°N, 11.3°E), which is situated in a rural area ~30 km from Munich.

A single set of measurements for all eight wavelengths required an observational period of the order of 1 min. On each day of the experiment about six such sets were taken at intervals, over a period of the order of an hour. Whenever possible, this was arranged to coincide in time with the lidar measurements. Values for $\tau_p(\lambda)$ were calculated from an average of all sets of data obtained on a particular day.

Fig. 3 shows the values for the aerosol optical depth as a function of wavelength for the three days. The behavior on 19 and 21 July was very similar, while the 20th showed a somewhat greater optical depth. In all cases the variation with wavelength is approximately linear with a slope of −1.6.

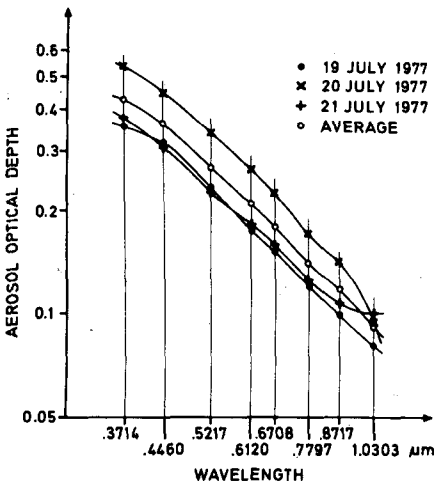

FIG. 3. Aerosol optical depth as a function of radiometer wavelength during the 3-day observational period.

This corresponds to a value of Junge's ν of 3.6 and is a fairly typical value for a continental aerosol (see, e.g., Reagan *et al.*, 1977).

e. Aerosol model used for interpretation

Analysis of radiometer data has been made in various ways, ranging from a simple analysis in terms of a Junge size distribution (Junge, 1963; Shaw *et al.*, 1973; Reagan *et al.*, 1977) to a full solution of the integral equations, relating extinction to aerosol particle parameters (King *et al.*, 1978; Yamamoto and Tanaka, 1969). This paper uses the bimodal log-normal distribution employed by Kent (1978). This model, although simple, approximates to the multimodal nature of aerosol size distributions, as pointed out by Whitby.[1] The model has two adjustable maxima, one in the accumulation mode (particle radii between 0.05 and 0.5 μm) and one in the coarse particle mode (particle radii between 2.5 and 25 μm). The other adjustable parameter, which controls the width of the log-normal curves (geometric standard deviation), has been given the value 2 suggested by Whitby. The optical extinction to be expected at each radiometer wavelength has been calculated for a family of log-normal curves with radii extending from 0.01 to 31.6 μm. The refractive indices used for these calculations are those given by Hänel and Bullrich (1978) for a continental clean-air aerosol. This varies from $1.54 - 0.013j$ at a wavelength of 0.37 μm to $1.49 - 0.02j$ at a wavelength of 1.03 μm. No account has been made of the effects of changes in humidity on these values which are not appreciable for values of humidity < 70%. The amplitude and position of the two maxima of the bimodal distribution is adjusted until the predicted optical depth at each wavelength matches the observed values for a given set of observations. Using a search procedure for the best fit, the parameters can usually be adjusted so that the rms deviation of the experimental optical depths from the predicted model values is only a few percent. As might be expected with more adjustable parameters, a better fit can usually be obtained than is possible using a Junge distribution. The model also possesses the advantage that figures can be obtained for the mass of aerosol in the accumulation and coarse particle modes, together with estimates of the accuracies of these figures. In general, using these radiometer wavelengths, it is found that the accumulation mode mass is determined fairly accurately but that the coarse particle mode mass may be in error by a large factor.

f. Experimental results

The model described above has been fitted to all the curves shown in Fig. 3. The following figures

[1] Whitby, K. T., 1973: On the multimodal nature of atmospheric aerosol size distribution. Presented at the VIII International Conference on Nucleation, Leningrad, U.S.S.R.

TABLE 2. Results of solar radiometer measurements. The radiometer values of backscattering cross section are very inaccurate, the vertically integrated values are much more accurate.

Date (July 1977)	Time (LST)	Aerosol vertical column mass: Accumulation mode (g m^{-2})	Aerosol vertical column mass: Coarse particle mode (g m^{-2})	Backscattering cross section β at 1.06 μm (m^{-1} sr^{-1})	Integrated vertical backscattering cross section β_R at 1.06 μm (sr^{-1})
19	1500–1630	0.070 (±15%)	indeterminate	2.38×10^4 (±60%)	15.4×10^{-4} (±30%)
20	1442–1513	0.100 (±10%)	zero	$3.48 \times 10^4 \begin{pmatrix} +5\% \\ -35\% \end{pmatrix}$	18.9×10^{-4} (±20%)
21	1430–1557	0.077 (±20%)	$0.289 \begin{pmatrix} +300\% \\ -100\% \end{pmatrix}$	$0.81 \times 10^4 \begin{pmatrix} +300\% \\ -100\% \end{pmatrix}$	$16.9 \times 10^{-4} \begin{pmatrix} +40\% \\ -20\% \end{pmatrix}$
Average					
19–21	1430–1630	0.081 (±10%)	$0.054 \begin{pmatrix} +150\% \\ -60\% \end{pmatrix}$	$2.42 \times 10^4 \begin{pmatrix} +60\% \\ -50\% \end{pmatrix}$	17.7×10^{-4} (±20%)

have been calculated for each day's experimental results and for the average of the three days:

1) The mass overload for the accumulation and coarse particle modes. For this the density figure of 1.86×10^3 kg m^{-3} given by Hänel and Bullrich has been used.

2) The theoretical lidar scattering cross section β_{180} at a wavelength of 1.06 μm. β_{180} is the predicted lidar scattering cross section per unit volume of aerosol (not aerosol-laden air). Its value is obtained by calculating the lidar scattering cross sections separately for the accumulation and coarse particle modes (using the fitted log-normal distribution and a refractive index of $1.49 - 0.02j$) and combining according to the relative concentrations of the two modes. The resultant value is an average over all heights (see Kent, 1978).

3) The integrated lidar scattering cross section $\beta_{180,R}$ for a vertical column through the atmosphere. $\beta_{180,R}$ is an estimate of the expected integrated lidar cross section for a unit area column and is given by

$$\beta_{180,R} = \beta_{180}\left(\frac{\text{aerosol mass overload per unit area}}{\text{aerosol particle density}}\right).$$

Limits of error for the theoretical and integrated cross sections are listed in Table 2. These limits are based on the goodness of fit of the models and represent the changes that would occur in the parameters if the model is altered so as to double the variance between the model predictions and the experimental values. They should be regarded as lower limits as they do not include errors in the model itself (incorrect refractive index or poor fit to actual particle size distribution) or errors in the experimental values. Nevertheless, they show that, as mentioned above, the accumulation mode mass is determined much better than the coarse particle mode mass and also that β_R is determined better than β itself.

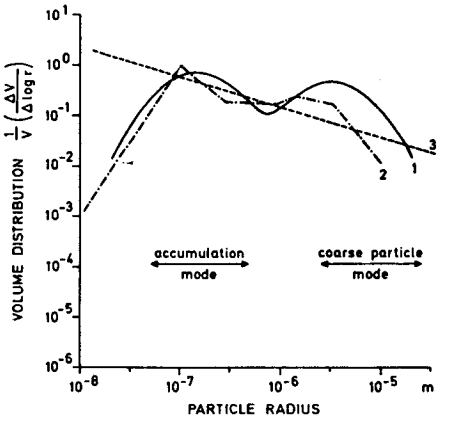

FIG. 4. Normalized volume distributions for (1) the best-fit model to the data for 19, 20 and 21 July 1977, (2) Hänel and Bullrich's continental clean-air aerosol, and (3) best-fit Junge distribution, $\nu = 3.6$ (not normalized).

Fig. 4 shows the particle size distribution for the best fit model to the average of three days data. The distribution has been plotted in terms of the particle volume rather than the particle number and is normalized so that the area under the curve is unity. Also plotted in the same graph are the corresponding curves for Hänel and Bullrich's continental clean air aerosol model and for the best-fit Junge distribution ($\nu = 3.6$). It can be seen how the fitted model shows the bimodal characteristic of the continental clean air aerosol distribution and agrees well with it for particle radii of less than a few micrometers.

TABLE 3. Comparison of lidar and solar radiometer results for 19–21 July 1977. β_A is the observed scattering cross-section per unit volume of *air*; β the theoretical value for unit volume of *aerosol* deduced from the radiometer data.

	Lidar data				Radiometer data		
Date (July 1977)	Time (LST)	Height range (m)	Mean β_A (m^{-1} sr^{-1})	Vertically integrated scattering β_R (sr^{-1})	Time (LST)	Value of β deduced from fitted model (m^{-1} sr^{-1})	Value of the vertically integrated scattering β_R from the atmosphere (sr^{-1})
19	16.09	0–1500	0.93×10^{-6}	14.0×10^{-4}	1500–1630	$2.38 \times 10^{4}\left(^{+60\%}_{-60\%}\right)$	$15.4 \times 10^{-4}\left(^{+30\%}_{-20\%}\right)$
20	14.15	0–1500	1.70×10^{-6}	25.5×10^{-4}	1442–1513	$3.48 \times 10^{4}\left(^{+5\%}_{-35\%}\right)$	$18.9 \times 10^{-4}\left(^{+20\%}_{-20\%}\right)$
21	14.33	0–1300	1.15×10^{-6}	15.3×10^{-4}	1430–1557	$0.81 \times 10^{4}\left(^{+300\%}_{-100\%}\right)$	$16.9 \times 10^{-4}\left(^{+40\%}_{-20\%}\right)$
Average 19–21			1.26×10^{-6}	18.0×10^{-4}		$2.42 \times 10^{4}\left(^{+60\%}_{-50\%}\right)$	$17.7 \times 10^{-4}\left(^{+20\%}_{-20\%}\right)$

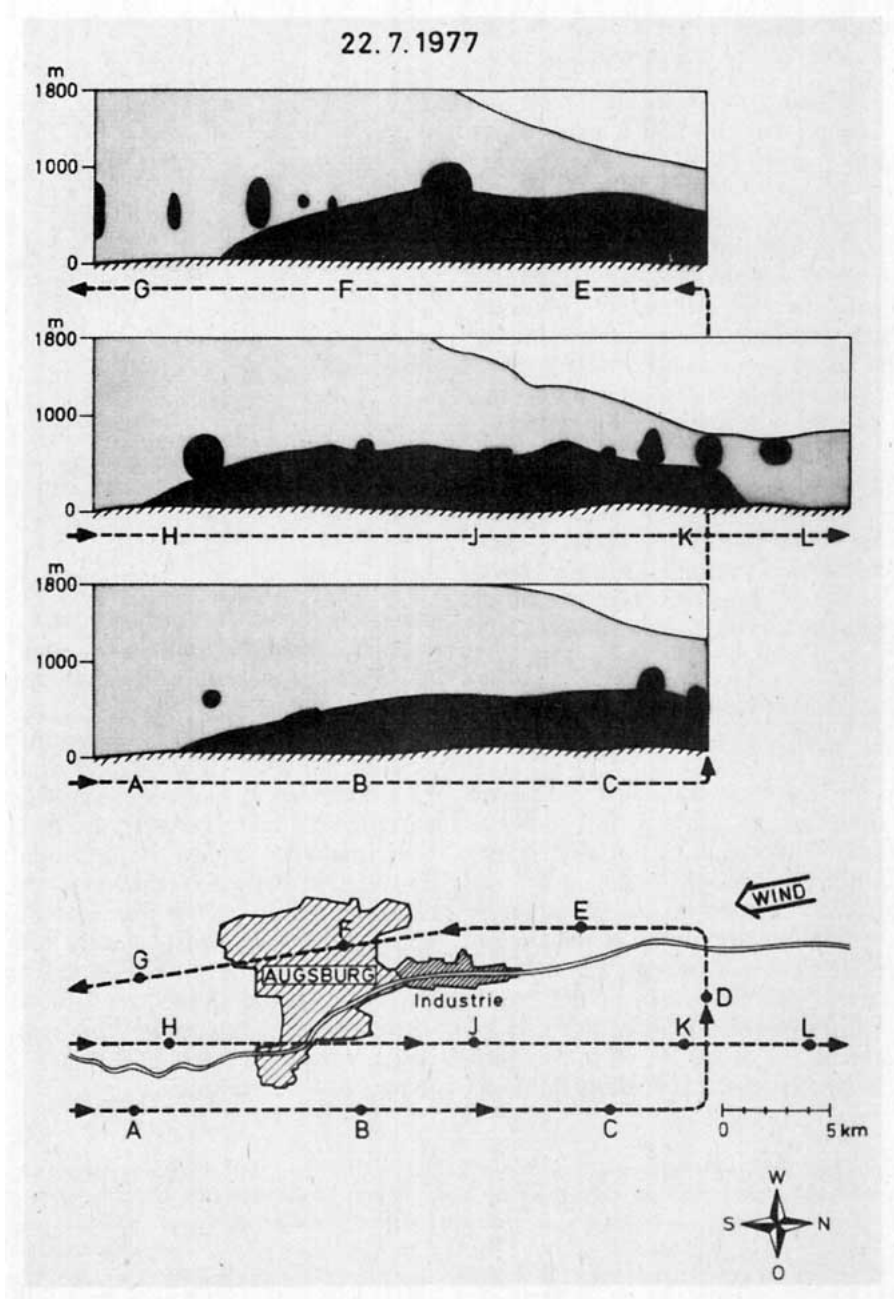

FIG. 5. Height/time cross section of the aerosol structure measured on 22 July 1977 over Augsburg area. The aerosol mass concentrations are represented by white: <150 μg m^{-3}; light grey: 150–225 μg m^{-3}; dark grey: >225 μg m^{-3}; black (clouds).

4. Comparison of lidar and solar radiometer results

In the last column of Table 2 the backscattering cross sections integrated over a vertical column through the whole atmosphere are given for the laser wavelength of 1.06 μm. These values have been derived from the radiometer data and will now be compared with the lidar measurements. For this purpose, the lidar profiles from the local overflights (Fig. 2) are integrated from the ground up to the inversion height. The results are listed in Table 3 together with the radiometer data.

Comparison of the lidar and the radiometer results shows fairly good agreement for each day and very good agreement for the average of the three days. Since most of the aerosol, but not the whole amount, lies within the integration boundaries from zero to 1500 m the lidar values would be expected

to be somewhat smaller than the radiometer values. For the same reason, the vertically integrated scattering from the lidar varies more for individual days than does the corresponding data from the radiometer. The extent of the difference depends on how much aerosol lies above 1500 m altitude.

5. Interpretation of airborne lidar aerosol measurements

One example of aerosol measurements by the airborne lidar system will be shown to demonstrate the applicability of this technique.

During the joint experiment a flight pattern over the Augsburg area was flown which covered regions of rural, urban and industrial character. All backscatter profiles taken have to be converted into profiles of mass concentration. Since we have no information on the actual properties of aerosol in this area, it is convenient to use the information on the aerosol particle size distribution given by the radiometer data at Oberpfaffenhofen (40 km southeast of Augsburg). Using these data, the backscattering cross sections β have been transformed into mass concentrations m, taking $\beta/m = 13.08$ m^2 sr^{-1} kg^{-1} as calculated from the radiometer measurements. (This value of β/m is really applicable only to the non-urban parts of the flight pattern and will be too great for the urban parts of the flight.) The resultant vertical profiles of mass concentration from the three north-south flight tracks are shown in Fig. 5 as separate height-time cross sections (A-C, E-G, H-L). Above the town of Augsburg and the industrial area north of it a layer of ~500 m thickness with relatively high mass concentration—represented by the dark-grey regions—can be seen. There, the aerosol mass decreases more or less continuously with increasing height. Only in the north can one observe a region with a low aerosol content—represented by the lightest patches. This may have been caused by the wind which was carrying clean air from the north, toward and over the Augsburg plume.

6. Conclusion

Airborne lidar measurements can be used to observe vertical layering and horizontal transport of aerosol masses. The transition from the lidar backscatter data to the quantitative aerosol mass concentration, unfortunately, contains some uncertainties. These are produced by the assumption of the properties of the aerosol models used for the calculations. The uncertainties of the method can be reduced if *in situ* measurements of aerosol properties are carried out at few places in the observed area. One simple method of improving the data is the use of a solar radiometer to provide information about the aerosol particle size distribution and total mass overload.

Acknowledgment. We are grateful to the Department of Electrical Engineering, University of Arizona, for the loan of the solar radiometer with which the measurements were made.

REFERENCES

Handbook of Geophysics and Space Environments, 1965: Air Force Cambridge Research Laboratories, St. Valley, Ed. (see pp. 7.1–7.36).

Hänel, G., and K. Bullrich, 1978: Physico-chemical property models of tropospheric aerosol particles. *Beitr. Phys. Atmos.*, **51**, 129–138.

Junge, C. E., 1963: *Air Chemistry and Radioactivity*. Academic Press (see pp. 111–202).

Kent, G. S., 1978: Deduction of aerosol concentrations from 1.06 μm lidar measurements. *Appl. Opt.*, **17**, 3763–3773.

King, M. D., B. M. Byrne, B. M. Hermann and J. A. Reagan, 1978: Aerosol size distributions obtained by inversion of spectral optical depth measurements. *J. Atmos. Sci.*, **35**, 2153–2167.

Reagan, J. A., J. D. Spinhirne, D. M. Byrne, D. W. Thompson, R. G. DePena and Y. Mamone, 1977: Atmospheric particulate properties inferred from lidar and solar radiometer observations compared with simultaneous *in situ* aircraft measurements: a case study. *J. Appl. Meteor.*, **16**, 911–928.

Shaw, G. E., 1976: Nitrogen diocide-optical absorption in the visible. *J. Geophys. Res.*, **81**, 5791–5792.

——, J. A. Reagan and B. M. Hermann, 1973: Investigations of atmospheric extinction using direct solar radiation measurements made with a multiple wavelength radiometer. *J. Appl. Meteor.*, **12**, 374–380.

Werner, Ch., F. Bachstein, S. Dietz, H. Herrmann, F. Köpp and H. Löffler, 1978: Airborne lidar aerosol measurements during the ASSESS II mission. *Rev. Sci. Instrum.*, **49**, 974–981.

Wilcox, R. W., G. D. Nastrom and A. D. Belmont, 1977: Periodic variations of total ozone and of its vertical distribution. *J. Appl. Meteor.*, **16**, 290–298.

Yamamoto, G., and M. Tanaka, 1969: Determination of aerosol size distribution from spectral attenuation measurements. *Appl. Opt.*, **8**, 447–453.